



Optical Proxies for Terrestrial Dissolved Organic Matter in Estuaries and Coastal Waters

Christopher L. Osburn^{1*}, Thomas J. Boyd², Michael T. Montgomery², Thomas S. Bianchi³, Richard B. Coffin⁴ and Hans W. Paerl⁵

¹ Department of Marine, Earth, and Atmospheric Sciences, North Carolina State University, Raleigh, NC, USA, ² Marine Biogeochemistry, US Naval Research Laboratory, Washington, DC, USA, ³ Department of Geological Sciences, University of Florida, Gainesville, FL, USA, ⁴ Department of Physical and Environmental Sciences, Texas A&M University, Corpus Christi, TX, USA, ⁵ Institute of Marine Sciences, The University of North Carolina at Chapel Hill, Morehead City, NC, USA

OPEN ACCESS

Edited by:

Marta Álvarez,
Instituto Español de Oceanografía,
Spain

Reviewed by:

Claire Mahaffey,
University of Liverpool, UK
Christian Lonborg,
Australian Institute of Marine Science,
Australia
X. Antón Álvarez-Salgado,
CSIC, Spain

*Correspondence:

Christopher L. Osburn
closburn@ncsu.edu

Specialty section:

This article was submitted to
Marine Biogeochemistry,
a section of the journal
Frontiers in Marine Science

Received: 04 October 2015

Accepted: 24 December 2015

Published: xx January 2016

Citation:

Osburn CL, Boyd TJ,
Montgomery MT, Bianchi TS,
Coffin RB and Paerl HW (2016)
Optical Proxies for Terrestrial
Dissolved Organic Matter in Estuaries
and Coastal Waters.
Front. Mar. Sci. 2:127.
doi: 10.3389/fmars.2015.00127

Dissolved organic matter (DOM) absorbance and fluorescence were used as optical proxies to track terrestrial DOM fluxes through estuaries and coastal waters by comparing models developed for several coastal ecosystems. Key to using these optical properties is validating and calibrating them with chemical measurements, such as lignin-derived phenols—a proxy to quantify terrestrial DOM. Utilizing parallel factor analysis (PARAFAC), and comparing models statistically using the OpenFluor database (<http://www.openfluor.org>) we have found common, ubiquitous fluorescing components which correlate most strongly with lignin phenol concentrations in several estuarine and coastal environments. Optical proxies for lignin were computed for the following regions: Mackenzie River Estuary, Atchafalaya River Estuary (ARE), Charleston Harbor, Chesapeake Bay, and Neuse River Estuary (NRE) (all in North America). The slope of linear regression models relating CDOM absorption at 350 nm (a_{350}) to DOC and to lignin, varied 5–10-fold among systems. Where seasonal observations were available from a region, there were distinct seasonal differences in equation parameters for these optical proxies. The variability appeared to be due primarily to river flow into these estuaries and secondarily to biogeochemical cycling of DOM within them. Despite the variability, overall models using single linear regression were developed that related dissolved organic carbon (DOC) concentration to CDOM ($\text{DOC} = 40 \pm 2 \times a_{350} + 138 \pm 16$; $R^2 = 0.77$; $N = 130$) and lignin (Σ_8) to CDOM ($\Sigma_8 = 2.03 \pm 0.07 \times a_{350} - 0.47 \pm 0.59$; $R^2 = 0.87$; $N = 130$). This wide variability suggested that local or regional optical models should be developed for predicting terrestrial DOM flux into coastal oceans and taken into account when upscaling to remote sensing observations and calibrations.

Keywords: CDOM absorbance, CDOM fluorescence, dissolved organic matter (DOM), lignin, carbon stable isotopes

INTRODUCTION

Terrestrial organic carbon (OC) flux from rivers and estuaries into coastal oceans is on the order of 0.2 Pg C yr^{-1} and constitutes a major part of the oceanic carbon cycle (Raymond and Spencer, 2014). Absorbing and fluorescing properties of chromophoric dissolved organic matter (CDOM) have been used to fingerprint OC sources, and often to track terrestrial DOM fluxes into the ocean (Coble, 2007). These optical properties can be used as proxies for organic matter in such instances to calibrate remote sensing observations from space and in deployed *in situ* platforms (Mannino et al., 2008; Fichot and Benner, 2011; Etheridge et al., 2014). In particular, ultraviolet (UV) absorption has been used to quantify DOC and measure its quality (sources) (Ferrari, 2000; Stedmon et al., 2000; Helms et al., 2008; Fichot and Benner, 2011; Asmala et al., 2012).

Studies on terrestrial DOC fluxes from rivers into coastal waters rely on strong correlations between DOC and lignin (e.g., Hernes and Benner, 2003; Spencer et al., 2008; Walker et al., 2009; Fichot and Benner, 2012). In terms of estuarine and coastal ocean biogeochemistry, this work has mainly been restricted to large rivers and to delta front estuaries (Raymond and Spencer, 2014). Both CDOM and lignin have been studied widely in estuaries separately, but rarely together (e.g., Osburn and Stedmon, 2011). This paucity of information complicates an understanding of how estuarine processes modify terrestrial DOC during transport to coastal waters.

In this work, we report on an analysis of CDOM, DOC, and lignin measurements from six estuaries across North America: the Atchafalaya River, the Mackenzie River, the Chesapeake Bay, Charleston Harbor, Puget Sound, and the NRE. These six systems represent a wide variety of estuaries in terms of their formation, morphology, hydrology, and their geographical distributions, as well as their catchment vegetation and land use. The aim of this work is to determine efficacy of using CDOM properties to predict DOC and lignin concentration across these six estuaries. Both CDOM absorption and excitation-emission matrix (EEM) fluorescence, modeled by parallel factor analysis (PARAFAC), were evaluated. Finally, we assessed whether optical-chemical linkages that underlie coupled optics-biogeochemical models can be applied widely across different estuarine types.

METHODS

Study Sites

Six North American estuarine and coastal systems were sampled from 2003 to 2011 (Table 1, Figure 1; station coordinates, Table S1). The Atchafalaya River Estuary (ARE) is a component of the Mississippi-Atchafalaya River System (MARS) a major component of the Gulf of Mexico. This river receives diverted flow from the Mississippi River and thus reflects the Mississippi's drainage. The Chesapeake Bay (CBE) is the largest estuary in the continental United States and the largest system we studied. The CBE has multiple river inputs and is heavily impacted by urban and agricultural land use. Charleston Harbor (CHE) is a coastal plain estuary dominated by three main river inputs (Ashley, Cooper, and Wando). The Mackenzie River (MRE) is one of the

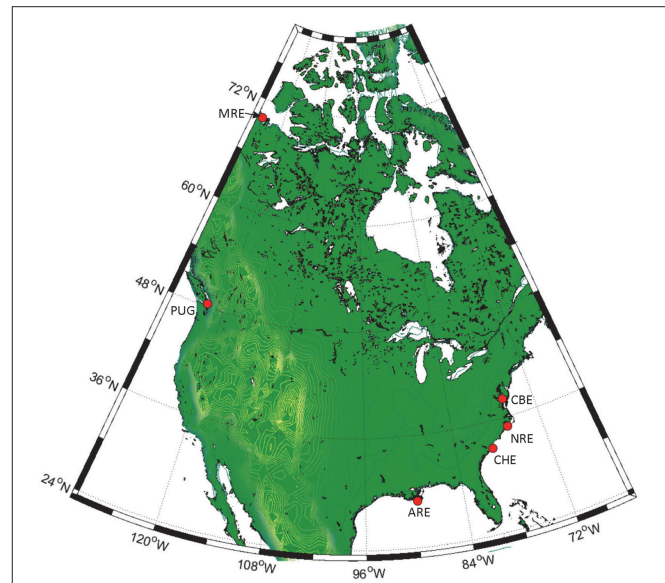


FIGURE 1 | Locations of the six North American estuaries in this study. Clockwise from right: Chesapeake Bay (CBE), Neuse River (NRE), Charleston Harbor (CHE), Atchafalaya River (ARE), Puget Sound (PUG), and Mackenzie River (MRE).

largest rivers flowing into the Arctic Ocean and drains boreal forest and Arctic tundra. The Neuse River Estuary (NRE) drains into the largest lagoonal estuary in the United States, the Pamlico Sound. The NRE receives drainage from the lower Piedmont to Coastal Plain and, like CBE, has had chronic problems with eutrophication. Puget Sound in the Pacific Northwest region of the United States contains several deep fjords (e.g., Hood Canal) and several small rivers. In this study, we includes samples from Hood Canal, the Snohomish River, and the Straits of Juan de Fuca, the latter which connect Puget Sound to the Pacific Ocean. Thus, our data set cover estuaries sampled across wide geographic and climatic regions.

There were more observations for the CBE and NRE than the other systems. Most observations came from estuarine environments although several samples came from coastal waters across the continental shelf (with the exception of Puget Sound). These seasonal samplings spanned a salinity range from 0 to 36. Thus, the data set represents a range of river influences from weak (Puget Sound) to strong (Atchafalaya and Neuse River Estuaries) and hence captures most hydrologic conditions encountered in estuaries. Only the NRE had a truly comprehensive seasonal dataset covering spring, summer, autumn, and winter. Most samples were collected from just below the water surface, though some were collected at mid-depths either by pneumatic pumps with Teflon tubing suspended at depth or by Niskin bottles. Salinity was often different for these sub-surface samples compared to their surface water counterparts so these samples were treated separately.

Two events of note for these samplings are important to mention. In July 2006, the Chesapeake Bay was sampled roughly 1 week after a period of intense summer squalls with increased freshwater discharge to the Bay. Discharge of the Bay's main

TABLE 1 | Site description information for the estuaries and coastal waters in this study.

Location	Code	Environment	Year(s) sampled	Season	No. of samples	Notes
Atchafalaya River	ARE	Delta front estuary	2007	Spring	7	Data include the Louisiana-Texas shelf and possibly influenced by the Mississippi River
			2011	Summer	14	Data are from Bianchi et al. (2011)
Chesapeake Bay	CBE	Coastal plain estuary	2004	Spring	12	Includes observations from the Potomac River and other major river mouths in the Chesapeake Bay
				Summer	7	
			2005	Spring	15	Samples collected after period of substantial rain the CBE watershed
			2006	Summer	8	
Charleston Harbor	CHE	Coastal plain estuary	2011	Summer	4	
Mackenzie River	MRE	Delta front estuary	2003	Summer	1	CDOM and DOC data from Osburn et al. (2009)
				Autumn	1	
			2004	Spring	4	
				Summer	12	
Neuse River	NRE	Coastal plain estuary	2010	Spring	9	
				Summer	5	
				Autumn	11	
				Winter	6	
				2011	Winter	
Puget Sound	PUG	Sound	2005	Autumn	8	Data include the Snohomish River, Dabob Bay, and the Straits of Juan de Fuca

tributary, the Susquehanna River, measured at Conowigo, MD, approached $11,000 \text{ m}^3 \text{ s}^{-1}$ (USGS gauge 01578310) and the Potomac River, measured near Washington, DC, approached $2300 \text{ m}^3 \text{ s}^{-1}$ (USGS gauge 01646502). Mean annual flows for each river (2000–2014) were 1184 and $346 \text{ m}^3 \text{ s}^{-1}$, respectively.

The second event occurred in the Atchafalaya River basin whereby a flooding event in May 2011 required that the Morganza Floodway near Baton Rouge, be opened for the first time in 40 years, to prevent New Orleans from being flooded. More specifically, the floodway was opened on May 14, 2011 when the Mississippi River reached a flow of over $42,000 \text{ m}^3 \text{ s}^{-1}$, the highest flow recorded since floods of 1927.

Optical Analyses

Absorbance and fluorescence were measured according to Osburn et al. (2009, 2012). Briefly, samples were filtered shipboard, refrigerated and analyzed within 3 weeks of each field effort. Absorbance (A) was measured on filtered samples, although two different filter sizes were used: $0.2 \mu\text{m}$ filters prior to 2009 and $0.7 \mu\text{m}$ filters after 2009. All samples were scanned from 200 to 800 nm against air and periodic MilliQ water blanks were scanned and subtracted from sample spectra. Samples were diluted if the absorbance in a 1-cm cell was greater than 0.4 at 240 nm. Absorbances at wavelength, λ , corrected for MilliQ water blanks were converted to Napierian absorption coefficients (a):

$$a(\lambda) = \frac{A(\lambda_{\text{sample}}) - A(\lambda_{\text{blank}})}{L} \times 2.303 \quad (1)$$

This study focused on absorption at 350 nm (a_{350}) to quantify CDOM absorption in comparison with previous work (Uher et al., 2001; Hernes and Benner, 2003; Lønborg et al., 2010; Spencer et al., 2013).

Two different fluorometers were used: a Shimadzu RFPC-5301 (samples before 2009) and a Varian Eclipse (samples after 2009). The time lag between their usages precluded intercalibration of their results, though the similarity in response to analyzing the same standards or to Raman unit scaling has been reported (Cory et al., 2010). However, data treatment for each instrument was the same. Standard corrections for lamp excitation and detector emission were applied, and afterward, corrections for the inner filter effects were applied. Scanning was performed with an excitation ranging from 250 to 450 nm (by 5 nm) and emission ranging from 300 to 600 nm by 1 nm resolution. Integration time on the RFPC-5301 instrument was 0.2 s (e.g., Boyd and Osburn, 2004). On the Varian instrument, scanning was performed with an excitation range from 240 to 450 nm in 5 nm increments and an emission range of 300 – 600 nm in 2 nm increments. Integration time on the Varian instrument was 0.125 s (Osburn et al., 2012). Shimadzu fluorescence results were resized in Matlab to match with Varian results over the excitation and emission wavelength ranges. Finally, the results were calibrated first to the water Raman signal of each instrument and then in quinine sulfate units (QSU). All fluorescence data were normalized to the total integrated fluorescence in each EEM prior to PARAFAC (Murphy et al., 2013).

DOC Analysis

Dissolved organic carbon (DOC) and $\delta^{13}\text{C}$ -DOC values were measured using wet chemical oxidation coupled with isotope ratio mass spectrometry (Osburn and St-Jean, 2007). Samples were acidified with 85% H_3PO_4 in the field (if not frozen) and stored in the dark until analysis. Samples were pre-sparged with ultrapure helium to remove inorganic carbon prior to analysis. WCO-IRMS system was calibrated daily with IAEA standards of glutamic acid, sucrose, oxalic acid, and caffeine. Routine analysis of the University of Miami Deep Sea Reference DOC (DSR) for this methodology produced DOC concentrations of $45 \pm 3 \mu\text{M}$ and $\delta^{13}\text{C}$ -DOC values of $-20.5 \pm 0.4\text{‰}$ ($N = 11$ for samples before 2008 and $N = 32$ for samples after 2008). Error on DOC concentrations by this method were $<3\%$ and reproducibility on $\delta^{13}\text{C}$ -DOC values was $\pm 0.4\text{‰}$.

Dissolved Lignin Analysis

Lignin was extracted from DOM via passage over C_{18} cartridges that were either assembled in the laboratory or purchased pre-assembled (Mega Bond Elut cartridges) (Louchouart et al., 2000; Kaiser and Benner, 2011). Samples were eluted from C_{18} cartridges with methanol, dried and oxidized to release lignin-derived phenols into solution. Microwave oxidation was used for all samples following Goñi and Montgomery (2000), except ARE samples from 2011, which used oven oxidation (Bianchi et al., 2013). Samples were then acidified, recovery standards added, then extracted into ethyl acetate and dried prior to

storage at 4°C . Prior to analysis, samples were re-dissolved into pyridine, derivatized with BSTFA+1% TMS, and then measured via gas chromatography-mass spectrometry. Calibration curves of 8 lignin derived phenols (vanillin, acetovanillone, vanillic acid, syringaldehyde, acetosyringone, syringic acid, p-coumaric acid, and ferulic acid) were used to quantify concentrations. Detailed methods for lignin analysis can be found in Osburn and Stedmon (2011), Bianchi et al. (2013), and Dixon (2014).

Statistical Analyses

Parallel factor analysis (PARAFAC) was conducted on EEMs from all estuaries in this study using the DOMFluor toolbox for Matlab (Mathworks, Natick MA) (Stedmon and Bro, 2008). Matlab statistical toolbox (releases spanning 2003 to present) was also used for other statistical tests. R^2 -values are adjusted values and significance of regression models was tested at $\alpha = 0.05$. Principle components analysis (PCA) was conducted using the PLS_Toolbox (Eigenvector, Inc., Seattle, WA) for Matlab. Autoscaling was used on variables measured prior to PCA.

RESULTS

Summary Statistics for Each System

CDOM, DOC, lignin, and (when available) $\delta^{13}\text{C}$ -DOC data for each system are summarized as boxplots (Figure 2) and presented in its entirety (Table S1). Note that $\delta^{13}\text{C}$ -DOC values were not available for ARE in summer 2011, and for some CHE

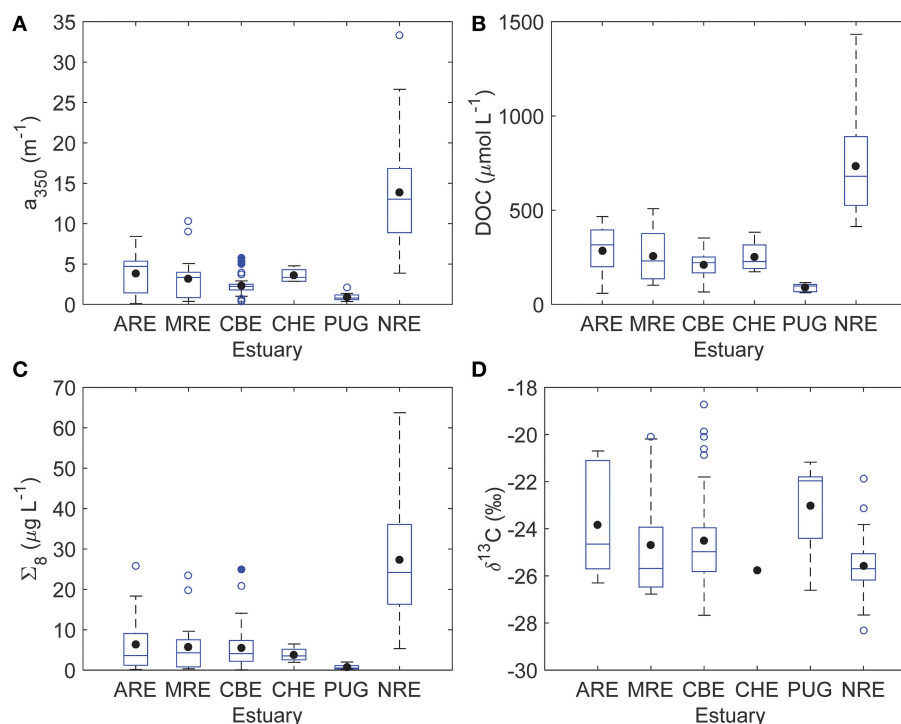


FIGURE 2 | Boxplots summarizing key variables measured for six estuaries in this study. **(A)** CDOM absorption at 350 nm (a_{350}); **(B)** DOC concentration; **(C)** sum of 8 lignin phenols (Σ_8); **(D)** stable carbon isotope values of DOC ($\delta^{13}\text{C}$ -DOC). The blue solid line is the median and the black circle is the mean; the edges of the boxes denote the 25th and 75th percentiles, while the whiskers denote the 10th and 90th percentiles, and blue circles represent outliers.

457 and NRE samples. Mean CDOM absorption at 350 nm (a_{350}) was
 458 highest for NRE (13.03 m^{-1}) and lowest for Puget Sound (0.90
 459 m^{-1}). The CBE and CHE estuaries had a_{350} values between 2 and
 460 3 m^{-1} and the ARE and MRE estuaries had a_{350} values between
 461 3 and 5 m^{-1} (Figure 2A). Mean DOC concentration for the NRE
 462 was 680 μM whereas for the other estuaries DOC averaged ca.
 463 250 μM (Figure 2B). PUG DOC values were overall the lowest of
 464 the data set and averaged 90 μM . The NRE also had the highest
 465 lignin concentration among the estuaries studied, with a mean
 466 Σ_8 of 24.2 $\mu g L^{-1}$, while PUG again had the lowest amount
 467 of lignin (mean $\Sigma_8 = 0.8 \mu g L^{-1}$) (Figure 2C). The mean Σ_8
 468 concentrations for CBE, CHE, ARE, and MRE ranged from 3.5 to
 469 4.3 $\mu g L^{-1}$. Both the CBE and NRE had more observations than
 470 other systems, especially CHE and PUG.

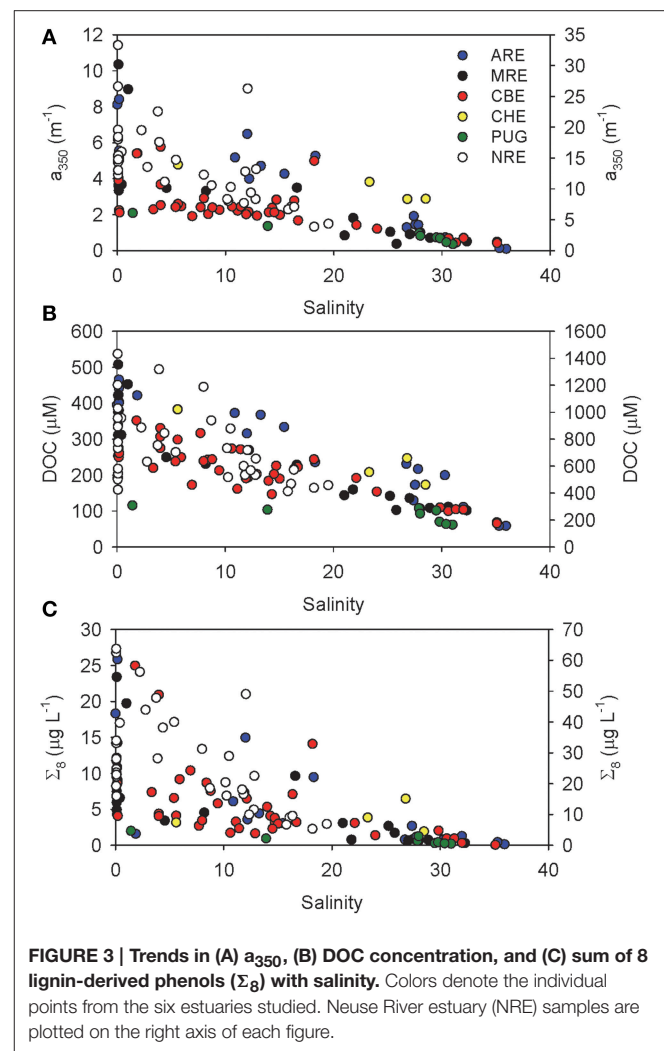
471 Stable carbon isotope values exhibited ranges common to
 472 estuarine environments and representing mixtures of terrestrial
 473 and planktonic organic matter (Figure 2D). Typically, riverine
 474 dissolved organic matter (DOM) values range from -26
 475 to -28‰ . By contrast, marine phytoplankton $\delta^{13}C$ values
 476 typically range from -22 to -18‰ , reflecting difference carbon
 477 fixation sources than land plants. Median $\delta^{13}C$ -DOC value
 478 was $-24.7 \pm 2.1\text{‰}$ which is typical of estuarine DOC (Bauer,
 479 2002; Bianchi, 2007). Median $\delta^{13}C$ -DOC values for MRE and
 480 CBE were -24.7 and -24.5‰ , respectively—close to median of
 481 the entire data set. Median $\delta^{13}C$ -DOC values for ARE and PUG
 482 were enriched at -23.8‰ and -23.0‰ respectively, suggesting
 483 more planktonic inputs. CHE only had one observation of $\delta^{13}C$ -
 484 DOM (-25.8‰). NRE had $\delta^{13}C$ -DOC values that were slightly
 485 depleted relative to the median at -25.4‰ . Further, this system
 486 exhibited the largest range of $\delta^{13}C$ -DOC values (-22 to -28‰)
 487 with the most frequent value of -26‰ .

488 Trends with Salinity

489 If coastal mixing between two end members (e.g., river and
 490 ocean) is conservative, chemical constituent concentrations
 491 plotted against salinity will exhibit a linear relationship.
 492 Deviations from conservative linear mixing are then interpreted
 493 to indicate biogeochemical cycling, for example, production or
 494 consumption of a chemical constituent or optical property. We
 495 examined trends in concentration of CDOM, DOC, and lignin
 496 against salinity for our entire dataset considering this simple
 497 mixing scenario. For the most part, linear trends with salinity
 498 were found, even for multiple river inputs in systems such as CBE
 499 (Figure 3). NRE had the lowest salinity range (0–20) but also the
 500 largest seasonal variability probably due to the higher resolution
 501 of sampling.
 502

503 Relationships Between CDOM Absorbance 504 and Fluorescence

505 Many studies of CDOM and lignin have used a_{350} to quantify
 506 CDOM absorption, so this convention was used for the
 507 remainder of the study with the understanding that primary
 508 CDOM absorption is caused by conjugated systems such
 509 as aromatic rings which have peak absorption near 254 nm
 510 (Weishaar et al., 2003; Del Vecchio and Blough, 2004). We chose
 511 a_{350} following on the work of Ferrari (2000) and Hernes and
 512 Benner (2003)—some of the first reported CDOM-DOC and
 513



514
515
516
517
518
519
520
521
522
523
524
525
526
527
528
529
530
531
532
533
534
535
536
537
538
539
540
541
542
543
544
545
546
547
548
549
550
551
552
553
554
555
556
557
558
559
560
561
562
563
564
565
566
567
568
569
570

FIGURE 3 | Trends in (A) a_{350} , (B) DOC concentration, and (C) sum of 8 lignin-derived phenols (Σ_8) with salinity. Colors denote the individual points from the six estuaries studied. Neuse River estuary (NRE) samples are plotted on the right axis of each figure.

CDOM-lignin relationships for coastal waters (Baltic Sea and Mississippi River plume, respectively). CDOM concentrations at a_{254} and a_{350} were highly correlated ($R^2 = 0.96$; $P < 0.0001$; $N = 130$).

The PARAFAC model we fit to our entire dataset produced four validated components, three of which exhibited humic-like fluorescence (C1–C3) and one which was amino acid-like (C4) (Figures 4A–D). Spectra for these components are presented along with results of the split-half validation (Figure S1). These components were matched against the OpenFluor database for similarity with up to 75 PARAFAC models from a range of aquatic ecosystems including boreal lakes, small and large rivers, estuaries, coastal, and open ocean water. Component 1 (C1) had excitation (Ex) maxima of 260 and 345 nm and emission (Em) maximum of 476 nm (Figure 4A). This component closely resembles soil-derived fulvic acids (Senesi, 1990). C2 had Ex/Em maxima of 310/394 nm and this component has been surmised as originating from microbial humic substances (Coble, 1996) (Figure 4B). C3 had Ex/Em of 250/436 nm and resembles humic substances (Figure 4C). C4 had Ex/Em of 275/312 nm which is situated between the fluorescence maxima of tyrosine and

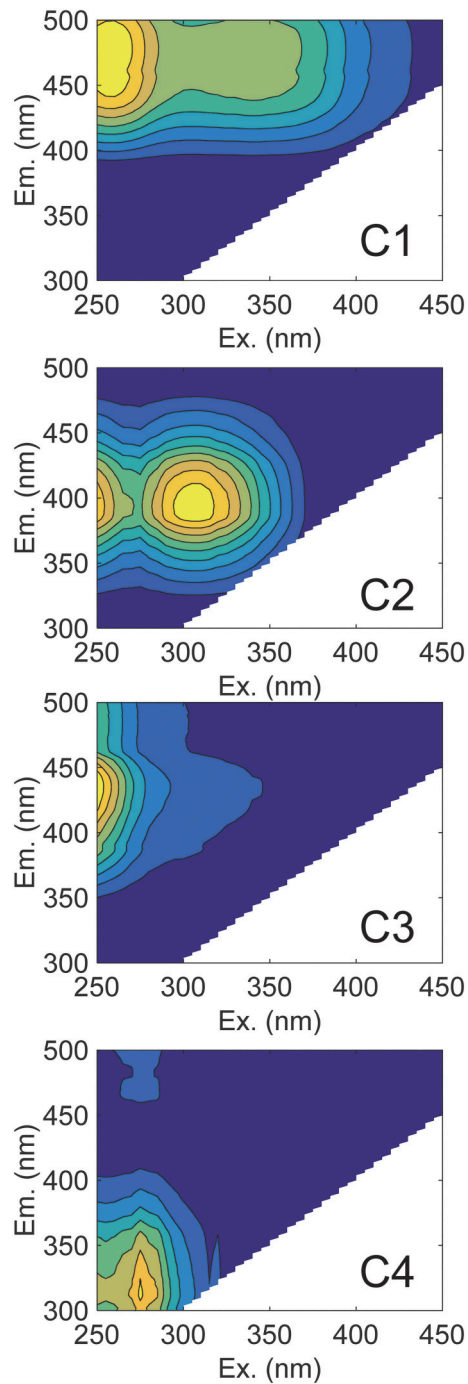


FIGURE 4 | EEM contour plots of the four PARAFAC components matched against the OpenFluor database. (A) C1 (soil fulvic acid); (B) C2 (microbial humic); (C) C3 (terrestrial humic); and (D) C4 (protein-like).

tryptophan, both of which are prevalent in natural waters (Wolfbeis, 1985; Figure 4D).

Of interest in this study were matches to our model components of those in river, estuaries, and coastal waters. Criteria for matching components were set at 95% similarity and assessed through Tucker's Congruence Coefficient via

TABLE 2 | Linear regression results between lignin concentration (Σ_8) and DOC concentration for four estuaries in this study.

Estuary	Slope	Intercept	R^2	P-value	N	Notes
ARE	17.4	69	0.99	< 0.001	7	Spring
MRE	18.2	81	0.98	0.005	4	Spring
CBE	46.6	101	0.71	< 0.001	17	2004 data
CBE	13.5	114	0.57	< 0.001	15	2005 data
CBE	8.8	143	0.84	< 0.001	8	2006 data
NRE	9.2	413	0.61	< 0.001	31	Outliers from winter and spring excluded (see text)

The linear regression equation was $DOC = \Sigma_8 \times Slope + Intercept$.

the OpenFluor database. Matches of each component with components from models in the database are also provided (Table S2). The maximum fluorescence intensity (FMax) values for C1 were most strongly corrected to a_{350} values over the entire dataset ($R^2 = 0.89$; $P < 0.001$). A stepwise multiple linear regression (MLR) was used to explore the importance of other components in explaining variation of a_{350} (data not shown). C2 was highly correlated to C1, while C3 only improved the model by <1%, which suggested their removal from the regression equation. C4 was not significant ($P = 0.126$).

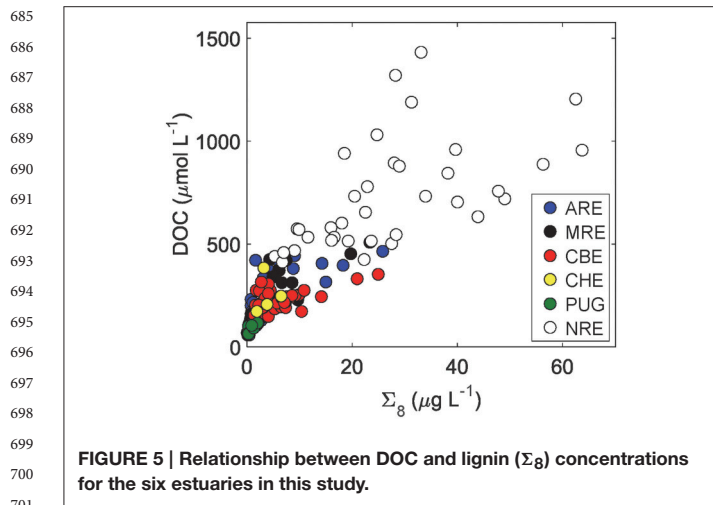
Relationships Between DOC and Lignin

DOC and lignin concentrations for the six estuaries showed a positive correlation ($DOC = 17.05 \pm 1.04 \times \Sigma_8 + 175 \pm 18$; $R^2 = 0.68$; $P < 0.001$; $N = 130$) (Figure 5). Although linear, the R^2 -value of this relationship suggests that roughly 30% of DOC was not explained by lignin concentration. Seasonal variability in these estuaries, observed in plots of DOC or lignin vs. salinity (Figures 3A–C), was evident in relationships between DOC and lignin for four estuaries where there were observations during more than one season (Table 2). Linear regressions for spring samplings in ARE and MRE produced correlation coefficients, R^2 , >0.9. By contrast, CBE and NRE had much weaker correlations: $R^2 = 0.57$ –0.84 for CBE and $R^2 = 0.61$ for NRE. CBE in particular showed seasonal variability represented as three regression lines for each of 2004, 2005, and 2006 were fit to the data and had much higher correlation coefficients than did the fit to all 3 years ($R^2 = 0.35$). For NRE, a linear fit to all values produced a correlation coefficient similar to CBE ($R^2 = 0.29$). DOC values >900 μM were excluded from NRE and the regression analysis re-ran, producing a much better fit ($R^2 = 0.61$; Table 2).

DISCUSSION

Predicting DOC and Lignin Concentrations in Estuaries and Coastal Waters Using CDOM

The major aim of this study was to determine the extent to which a cross-system optical-biogeochemical model for DOM could be developed for hydrologically-variable estuaries. We

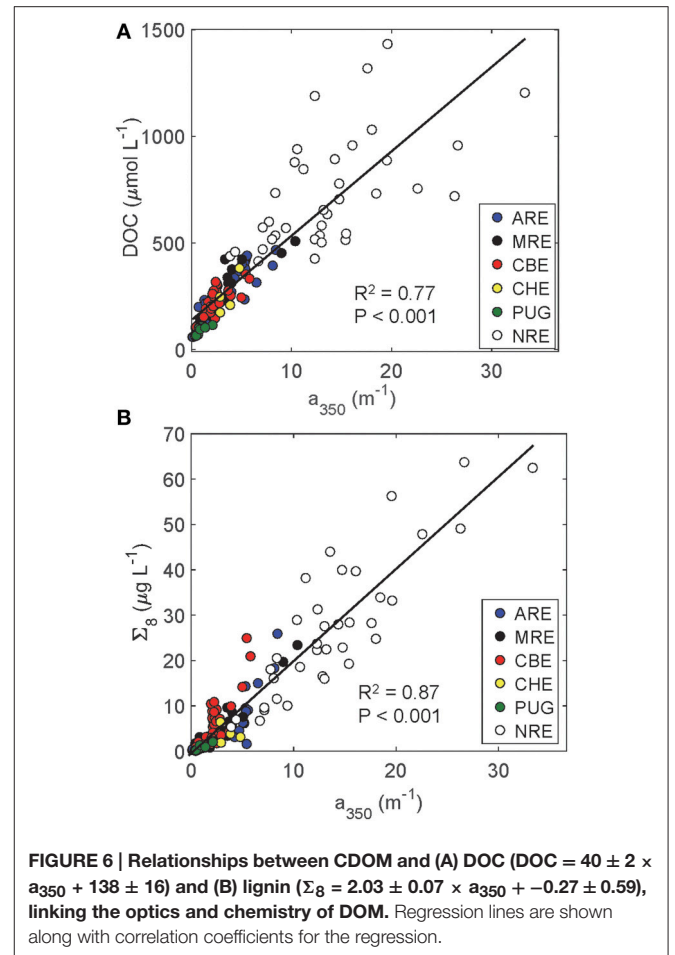


702
703 anticipated that the variability of estuarine ecosystems would
704 complicate the robustness of one simple model to describe
705 DOC or lignin concentrations across a gradient of estuaries
706 and adjacent coastal waters. Using simple linear regression, we
707 found that CDOM concentration measured at 350 nm explained
708 greater than 70% of the variance both in DOC and dissolved
709 lignin concentrations (Figures 6A,B). The higher correlation
710 coefficient for the CDOM-lignin model than the CDOM-DOC
711 model suggested that CDOM is generally terrestrial in many
712 different estuaries. Results from the Mississippi River plume and
713 boreal estuaries support this suggestion (e.g., Hernes and Benner,
714 2003; Asmala et al., 2012).

715 In fact, a_{350} serves as an excellent optical proxy for DOC for
716 many estuaries as seen for North American rivers (Spencer et al.,
717 2012). In that study, the authors showed consistent patterns of
718 strong linear trends between a_{254} and DOC and a_{350} and DOC
719 (see their Figure 5). That result was consistent with the linear
720 relationship between a_{350} and DOC found for the estuaries in this
721 study ($R^2 = 0.77$; $P < 0.001$; $N = 130$). Regression of DOC
722 on a_{254} values produced similar results ($R^2 = 0.76$; $P < 0.001$;
723 $N = 130$). Thus, it appears that general trends between optics
724 and chemistry can be modeled with some certainty.

725 CDOM absorption at a_{350} also was an excellent proxy for
726 lignin for the six estuaries we studied ($R^2 = 0.87$; Figure 6B).
727 Using a_{350} , Hernes and Benner (2003) found higher R^2 -values
728 (0.98) for the Mississippi River plume, but their model was only
729 for one sampling in May 2000. Fichot and Benner (2012) found
730 positive linear relationships for lignin vs. a_{350} for the Mississippi
731 River Plume in all seasons over 2009-2010 (R^2 -values ranged
732 from 0.89 to 0.99) and noted a seasonality in the slope coefficients
733 for these relationships.

734 Intercepts of these types of regressions should be interpreted
735 with some caution (Stedmon and Nelson, 2014). For the CDOM-
736 DOC relationship, the y-intercept value ($139 \mu\text{M}$ DOC) was
737 significantly different from zero ($P < 0.001$). This would suggest
738 that non-CDOM DOC in these estuaries approximates $140 \mu\text{M}$
739 but one must be careful in that these regressions are sensitive to
740 seasonality and hydrology (see below discussion on seasonal and
741 episodic variability). While Fichot and Benner found a robust



774
775 CDOM-DOC and CDOM-lignin models for the Mississippi
776 River plume, variability in regression statistics for CDOM-DOC
777 models in Finnish boreal estuaries led to the suggestion that
778 regional or sub-system models might be necessary (Asmala et
779 The latter study's results were consistent with the findings for the
780 North American estuaries in this study.

781 782 783 784 785 786 787 788 789 790 791 792 793 794 795 796 797 798

Fluorescence Indicated Dominant Influence of Terrestrial Sources of CDOM in Estuaries and Coastal Waters

799 Although CDOM absorption was a strong predictor for DOC
800 and lignin, PARAFAC of EEM fluorescence provides a powerful
801 means of characterizing DOC sources and prior work has shown
802 good correspondence between fluorescence and lignin (Amon
803 et al., 2003; Walker et al., 2009; Osburn and Stedmon, 2011)
804 but also has identified planktonic fractions (Zhang et al., 2009;
805 Romera-Castillo, 2011; Osburn et al., 2012). For example, a
806 fluorescence component similar to our C3 was found to be
807 important for predicting terrestrial DOM flux from the Baltic
808 Sea though (Osburn and Stedmon, 2011). Combining that
809 component with a protein-like component similar to our C4,
810 those authors estimated terrestrial DOC flux from the Baltic
811 Sea using multiple linear regression (MLR). Recently, Osburn

et al. (2015) applied the same fluorescence-based approach to modeling DOM dynamics in a small tidal creek system and found very strong relationships between fluorescence and DOM ($R^2 > 0.9$). Thus, we were interested in determining how this PARAFAC model, based on six estuaries (but weighted toward the CBE and NRE in terms of the numbers of samples), would perform with respect to identifying markers for terrestrial DOC (as lignin) and for planktonic DOC (as amino-acid like fluorescence, Osburn and Stedmon, 2011).

For this determination, stepwise MLR was run in a forward mode in which only positive coefficients with $P < 0.05$ were allowed to enter the model. The rationale was that to be predictive, fluorescence signals should have a positive relationship with lignin or with DOC. For lignin, we found that FMax values for C1 predicted about 82% of variability in Σ_8 values ($\Sigma_8 = -1.18 + 2.048 \times \text{FMaxC1}$; $P < 0.001$; $n = 130$). The intercept was not significant. C2 had a negative coefficient and was excluded which is sensible because this component matched with microbial humic substances. C3 was not significant in the model and C4 only increased the variance explained by about 1%. Therefore, C1 served as our terrestrial DOM marker.

C1 matched with 7 models on the OpenFluor database—all suggestive of terrestrial humic substances. This component's longwave emission properties (e.g., >450 nm) likely result from highly conjugated aromatic material and resemble isolated fulvic acids from soils and sediments (Senesi, 1990). C4 shared spectral features with 8 models on the OpenFluor database from estuarine and marine environments and, in each case, this component was attributed to protein-like or amino acid-like fluorescence. However, using partial least squares regression, Hernes et al. (2009) was able to demonstrate that fluorescence centered as Ex/Em wavelengths near our C4 was best predictive of lignin concentration. That result was not surprising given that lignin phenols originate as the fluorescent aromatic amino acid phenylalanine (Goodwin and Mercer, 1972), but does indicate the care that must be taken in calibrating fluorescence signals for prediction of chemical quantities. With this consideration in mind we next attempted stepwise MLR to use FMax values from the PARAFAC model to predict DOC concentrations in these estuaries.

MLR produced the following model:

$$\text{DOC} = 82.05 \times \text{FMaxC1} - 112.53 \times \text{FMaxC2} + 11.99 \times \text{FMaxC3} + 38.88 \times \text{FMaxC4} + 163.70 \quad (2)$$

FMax values for all components were significant in the model (Table 5). C1 explained the most variance. The coefficient for C2 was negative, which meant that as C2 fluorescence increased, DOC concentration decreased. This result suggested consumption of DOC by bacteria, and is consistent with the removal of terrestrial DOC in estuaries by bacteria (Moran et al., 2000; Raymond and Bauer, 2000; McCallister et al., 2004). C3 and C4, while significant, were less important in terms of their explanatory power in the model. Thus, as expected, the strongest linkage between optics and chemistry in the DOM of these six estuaries of this study was due to terrestrial organic matter. Overall, the MLR model demonstrated the importance of

terrestrial organic matter as a dominant component of the DOC in these estuaries.

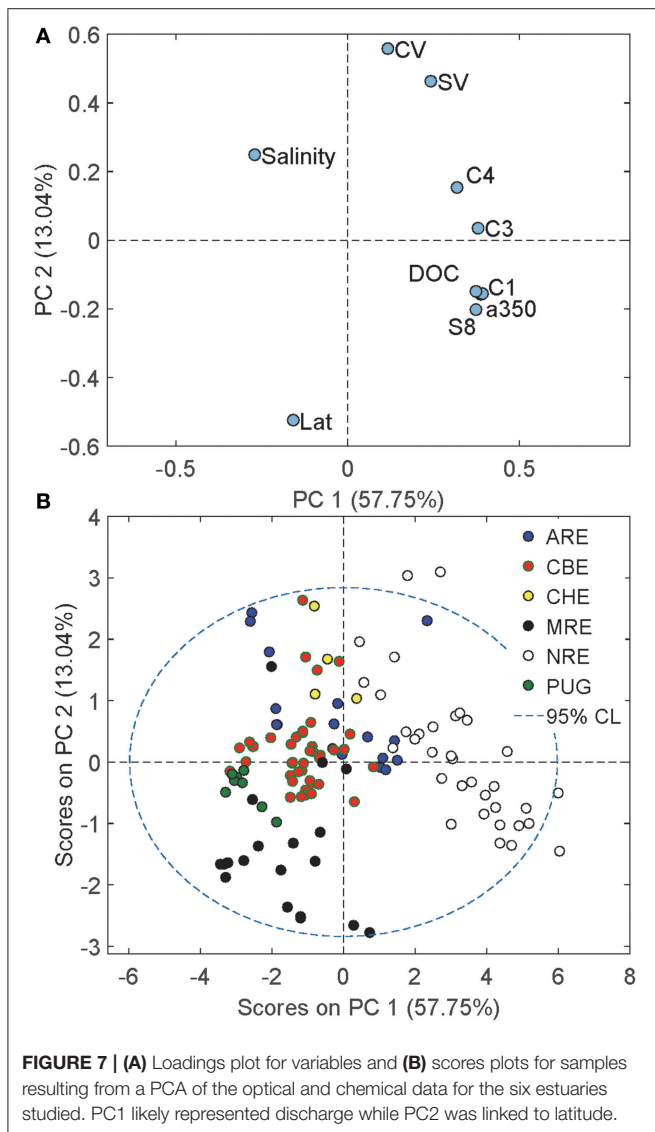
However, none of our four PARAFAC components matched to the Osburn and Stedmon (2011) model components which underscores the uncertainty in using fluorescence and provides a clear example of the considerations needed when using this approach. Universal models of fluorescence as a means to quantify DOC sources are likely unattainable because fluorescence properties are sensitive to biogeochemistry. For example, photodegradation is well known to cause proportionally more loss of fluorescence at longer excitation and emission wavelengths that arise from the conjugation and aromaticity that typify terrestrial CDOM sources (Boyle et al., 2009; Gonsior et al., 2009). Biodegradation, independently and in conjunction with photodegradation, can also cause a variety of spectral changes to fluorescence (Miller and Moran, 1997; Boyd and Osburn, 2004; Stedmon and Markager, 2005). Given the dynamics within and among estuaries, it is not surprising that our fluorescence results performed less well on hydrologically-variable estuaries than did those of Osburn and Stedmon (2011) which focused on one estuarine system. It is thus recommended that PARAFAC be limited to local or perhaps regional modeling of estuarine DOM.

Geographic Variability in CDOM-Lignin Relationships for Estuaries and Coastal Waters

The above discussion suggested ways in which both CDOM absorption and fluorescence could be utilized to link optical and chemical properties of estuaries and coastal waters both in terms of quantification (absorption) and estimates of DOM sources (fluorescence). PCA was then utilized to explore the optical and chemical data of these six estuaries with respect to each other (Figure 7). Ratios of syringyl lignin to vanillyl phenols (S:V) and ratio of cinnamyl to vanillyl phenols (C:V) were included in this analysis to identify plant tissue sources. FMax values for C2 were removed from the analysis because of the high correlation with C1. A 2-component PCA model explained 70% of the variance in these data.

Loadings for optical and chemical variables measured for these six estuaries showed interesting separation that supports the strong connection between CDOM and lignin in them (Figure 7A). Loadings for C1, a_{350} , DOC, and Σ_8 all clustered tightly in the lower right quadrant of the plot, closer to the PC1 axis than the PC2 axis and opposite of the loading for salinity. This result supports the concept that control of DOC and CDOM in these six estuaries was due to freshwater sources of terrestrial organic matter in rivers flowing into them. PC1 thus may be strongly tied to river flow; all CDOM, but especially C3, align with this axis.

Loadings for latitude and C:V and S:V ratios align most closely with PC2 and suggested some geographic influence on the DOM quality across these estuaries. Loadings for latitude were strongly negative on PC2 while loadings for S:V and C:V were strongly positive on PC2. This result was sensible because vegetation in lower latitudes typically has much more angiosperms than the gymnosperms that dominate boreal and Arctic environments.



Lignin quality across broad geographic gradients typically is reflected in these ratios (Onstad et al., 2000; Amon et al., 2012).

Scores for our samples clearly support the trends with freshwater (PC1) and with latitude (PC2) (Figure 7B). Scores for NRE were most positive on PC1 and NRE was the most freshwater dominated estuary of those in this study, with the highest CDOM, DOC, and lignin concentrations. By contrast, MRE had the most negative scores on PC2 reflecting the dominance of lignin in NRE by conifers which are depleted in cinnamyl phenols and thus C:V ratios are near zero. Similarly PUG scores were negative on PC2 representing the influence of mainly coniferous vegetation around the PUG and Snohomish River watersheds. However, CBE fell near the mean of the data set likely reflecting large land use gradients in its watershed of this temperate estuary.

The PCA suggested PARAFAC provided little distinction between these estuaries which was consistent with a recent study of Arctic rivers (Walker et al., 2013). However, C4 fluorescence

was more closely related to plant tissue type as indicated by loadings FMax values for C4, S:V, and C:V ratios that were positive both on PC1 and PC2. This could indicate that these lower latitude estuaries have more angiosperm and non-woody tissue producing this signal (Hernes et al., 2007). For example, tidal pulsing exported higher molecular weight, more aromatic and CDOM-rich marsh-derived DOC to the Rhode River sub-estuary of CBE (Tzortziou et al., 2008). Therefore, we may expect that more lignin also was exported from the marshes adjacent to the estuaries we studied. Most of our study sites were in temperate climates dominated by *Spartina* marsh plants—angiosperm grasses which would be enriched both in syringyl (S) and cinnamyl (C) phenols relative to vanillyl (V) phenols. Alternatively, these lower-latitude systems might coincidentally be more productive than the higher latitude systems. For example, one caveat to our results suggesting C4 is correlated to plant tissue type is that an unequal number of observations were made across six different systems and data for these cross-system regressions were dominated by CBE and NRE—both meso- to eutrophic estuaries (Paerl et al., 2006).

Seasonal and Episodic Variability in Optical Proxies for DOM within Specific Estuary Types

Fichot and Benner (2014) have developed remarkably consistent models relating CDOM absorption to lignin phenol concentration in surface waters from a large delta front estuary system we examined in this study, the MARS, of which ARE is a component. They noted seasonal variability of DOM in freshwater end members of these large river systems, and attributed most of that to seasonal variability in discharge. Asmala et al. (2012) also found substantial variability in CDOM-DOC relationships for boreal estuaries. The Mississippi-Atchafalaya system is similar to the MRE whereas the boreal estuaries were similar to the coastal plain-type estuaries, NRE and CBE.

The strongest control on CDOM and DOC in the estuaries we studied was river flow, which contributed CDOM-rich terrestrial DOM to these estuaries and their coastal waters. This was evident because of the linear relationship between CDOM and DOC and CDOM and lignin that we found across multiple estuary types (Figures 6A,B). For the CDOM-lignin relationship, the y-intercept value ($-0.50 \mu\text{g L}^{-1}$) was not significantly different from zero ($P = 0.503$). This result suggested that the vast majority of CDOM in these estuaries originated from terrestrial sources. CDOM absorption at wavelengths $>300 \text{ nm}$ is primarily due to conjugated molecules such as lignin (Del Vecchio and Blough, 2004). Therefore, it makes sense that in estuaries and coastal waters where rivers and coastal wetlands contribute DOM, this material will be highly conjugated and chromophoric (Raymond and Spencer, 2014).

Variable hydrologic regimes are well known to influence concentrations and relationships of CDOM, DOC and lignin in rivers and this certainly appears the case in many estuaries (Hernes et al., 2008; Saraceno et al., 2009; Spencer et al., 2010). For example, both CDOM and DOC doubled in concentration

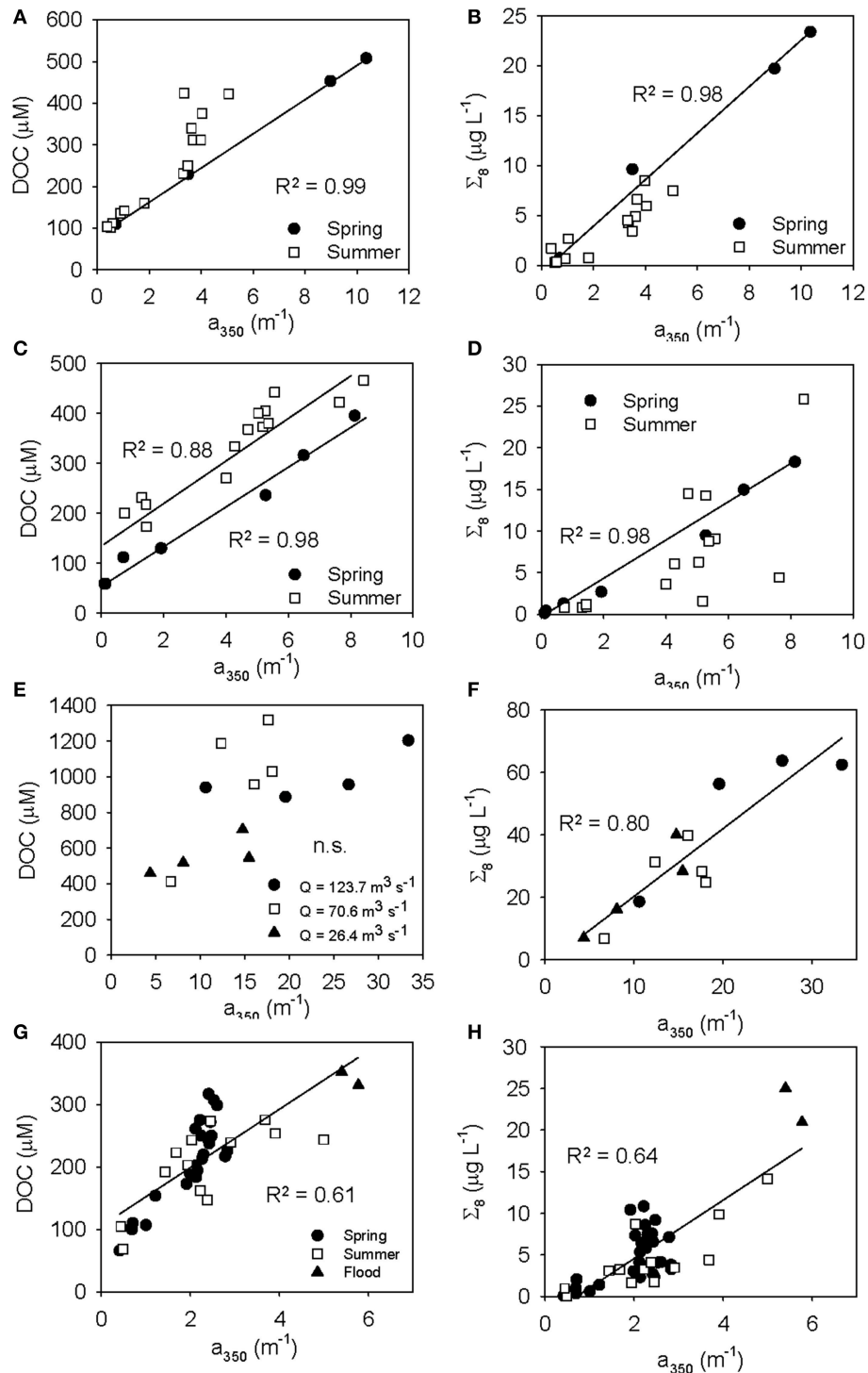
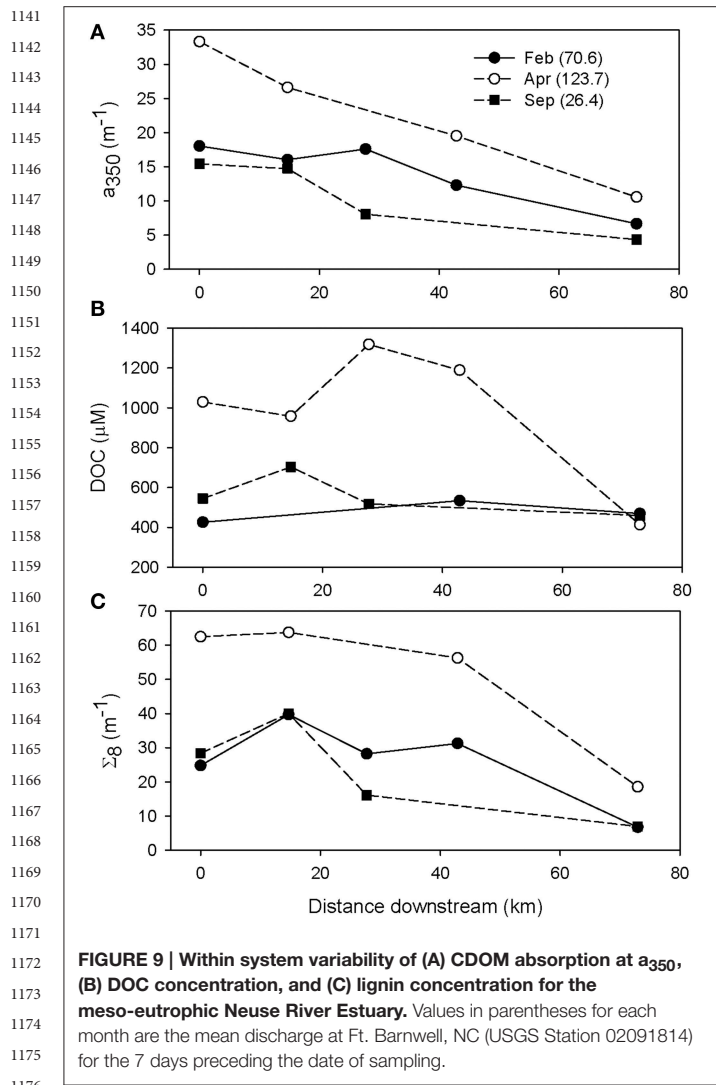


FIGURE 8 | Relationships between CDOM and (A) DOC and (B) lignin linking the optics and chemistry of DOM, influenced by hydrologic variability.

(A,B) MRE showing influence of spring freshet, (C,D) ARE showing influence of 2011 Mississippi River flood, (E,F) NRE showing seasonal influence of river discharge, and (G,H) CBE showing the influence of heavy rains in summer 2006. Significant linear regressions are shown while slope and intercept values and regression statistics are in Table 3. For (F–H), the regressions were fit to all of the data.

during the flushing hydroperiod of the tropical Epulu River (NE Congo) compared to the post-flush period, while Σ_8 values

tripled (Spencer et al., 2010). Discharge values for the major rivers flowing into the MRE, ARE, NRE, and CBE are listed in Table S3.



We found corroborating evidence of hydrologic variability in optical-biogeochemical models within estuaries for ARE, MRE, CBE, and NRE that was seasonal and episodic (Figures 8A–H). We do not extend our analysis of relationships beyond linear regression models as Fichot and Benner (2014) have done for DOC-normalized results; rather, we focus on the basic CDOM, DOC, and lignin measurements that can be used in a first order optical algorithm for satellite retrievals of properties related to ocean color (Mannino et al., 2008; Tehrani et al., 2013). These are expressed as either DOC or Σ_8 as a function of a_{350} . Further some concern about collinearity of the Fichot and Benner models has been raised (Asmala et al., 2012). Our subsequent analysis of seasonal trends exclude CHE and PUG for which we have too few observations.

For MRE, spring and summer distinctions were clear in the relationships between CDOM and DOC or CDOM and lignin that coincided with the spring flush of freshwater from Arctic rivers (Table 3 and Table S3). For example, in MRE, far more CDOM, DOC, and lignin were found in June just after the freshet as opposed to late August when the river had returned to base

flow (Figures 8A,B). This pattern is common of Arctic rivers which deliver the majority of DOM during the freshet (Amon et al., 2012). Larger concentrations of Σ_8 during spring indicates that this also is the case for ARE. Spring meltwaters in the upper Midwest US might similarly create a freshwater pulse leading to high discharge of the entire Mississippi-Atchafalaya system as suggested by the results of Fichot and Benner (2012). Therefore, in LDEs the large river flow forcing in these systems and could exhibit seasonally predictable patterns.

In contrast to ARE and MRE, which are both large delta front estuaries that extend well into coastal waters, NRE is a smaller, microtidal system with a long residence time between 20 and 120 days (Pinckney et al., 1998). However, like ARE and MRE, NRE is heavily riverine influenced, though this estuary exhibited a 3-fold range in CDOM, DOC, and lignin concentrations at the freshwater end member (Figure 3; Table S1). Variability of the NRE data around the regression line describing the general CDOM-DOC relationship we found for the estuaries in this study was the greatest and suggested some change in either the source or quality of DOM entering the NRE annually (Figure 6A).

The influence of discharge on CDOM, DOC, and lignin patterns across the NRE was further investigated (Figures 9A–C). River discharge to the NRE at Ft. Barnwell, NC, (USGS Station 02091814) was averaged for the 7 days prior to the sampling date on which the observations were made (Table S3). It was clear that high river flow contributed more CDOM, DOC, and lignin into the NRE than at lower flow. At lower flows ($Q = 26\text{--}70\text{ m}^3\text{ s}^{-1}$) CDOM decreased downstream but DOC and lignin were rather constant. This pattern changed substantially when $Q = 123.7\text{ m}^3\text{ s}^{-1}$ at Ft. Barnwell and concentrations of CDOM in the NRE doubled whereas concentrations of DOC and lignin nearly tripled. Thus, it is not surprising that the NRE data, which are roughly monthly over a 12-month period, captured the variability in high and low flow regimes. The change in DOM quality was somewhat larger than the load of terrestrial DOM as evidenced by the higher R^2 -value of the CDOM-lignin relationship as opposed to the CDOM-DOC relationship (Figures 6A,B).

In addition to seasonal variability, we had two examples of episodic loadings of terrestrial DOM into estuaries from high periods of rainfall that also contributed to deviations from general trends found in this study. In summer 2011, a flood in the Mississippi River basin delivered historically higher amounts of DOC to the coastal Gulf of Mexico (Bianchi et al., 2013). This resulted in large amounts of CDOM and lignin, as well (Figures 8C,D). Overall DOC concentrations were higher, illustrating how climate can perhaps increase the transfer of terrestrial DOC to coastal waters (Table 3). Other work in the northern Gulf of Mexico has shown that coastal marshes are a significant source of dissolved lignin to the estuaries and very shallow inner shelf regions (Bianchi et al., 2009), but not likely to the broader shelf areas (Fichot et al., 2014). Coastal marsh DOM could be mobilized as well during storm events. Large loads of terrestrial DOM have been shown to be delivered to the NRE by its watershed during tropical storms (Paerl et al., 1998; Osburn et al., 2014).

In June 2006, summer squalls produced heavy rainfall in the mid-Atlantic United States leading to 6- to 10-fold higher river

TABLE 3 | Parameter estimates (Est.) for linear regression models (DOC or $\Sigma_8 = m \times a_{350} + b$).

Estuary	Season	DOC	Est.	SE	adj R^2	P-value	Σ_8	Est.	SE	adj R^2	P-value
MRE	Spring	b	82	2	0.99	<0.001	b	0.22	1.27	0.98	0.881
MRE	Spring	m	41	1		<0.001	m	2.24	0.18		0.006
MRE	Summer	b	68	25	0.84	0.017	b	-0.21	0.65	0.79	0.751
MRE	Summer	m	69	8		<0.001	m	1.55	0.22		<0.001
ARE	Spring	b	59	11	0.98	<0.001	b	-0.52	0.62	0.98	0.442
ARE	Spring	m	39	2		<0.001	m	2.24	0.14		<0.001
ARE	Summer	b	181	35	0.87	<0.001	b	-0.74	3.04	0.37	0.813
ARE	Summer	m	29	3		<0.001	m	1.49	0.63		0.013
NRE	Spring, Summer, Autumn	b	477	153	0.35	0.010	b	-1.46	5.48	0.80	0.795
NRE	Spring, Summer, Autumn	m	24	9		0.019	m	2.17	0.31		<0.001
NRE	All	b	403	88	0.32	<0.001	b	-1.79	3.15	0.74	<0.001
NRE	All	m	24	6		<0.001	m	2.10	0.21		<0.001
CBE	Spring	b	44	20	0.74	0.034	b	-0.19	1.53	0.29	0.900
CBE	Spring	m	81	9		<0.001	m	2.47	0.72		0.002
CBE	Summer	b	117	27	0.49	0.001	b	-1.29	1.49	0.61	0.406
CBE	Summer	m	36	10		0.005	m	2.47	0.56		0.001
CBE	All	b	105	15	0.61	<0.001	b	-2.47	1.04	0.64	0.02
CBE	All	m	46	6		<0.001	m	3.51	0.41		<0.001

"SE" is the standard error of the regression parameter, "adj R^2 " is the adjusted correlation coefficient for the regression. "All" means the regression was carried out for all season (NRE and CBE only).

discharges to the CBE (Table S3). We had two observations each of CDOM, DOC, and lignin in the Potomac River, a sub-estuary of CBE, to provide a contrast of terrestrial DOM inputs between spring and summer (Figures 8G,H). These observations are titled "Flood" Figures 8G,H and demonstrate proportionally higher amounts of CDOM per unit DOC and lignin, respectively. These observations underscore the higher CDOM, DOC, and lignin values observed in the freshwater inputs to CBE (Figures 3A–C).

Finally, episodic variability in CDOM-DOC relationships for some estuaries could be linked to autotrophic sources of DOM within estuaries. NRE and CBE experience periodic, yet chronic, eutrophication caused by excessive nitrogen loading from their watersheds (Paerl et al., 2006; Paerl, 2009). Primary production from algae can add DOC to the estuary but not lignin. Phytoplankton-derived, and microbially-transformed, sources of CDOM have been documented for many estuaries and coastal waters though uncertainty in the magnitude of this source exists (Stedmon and Markager, 2005; Romera-Castillo et al., 2011; Osburn et al., 2012; Stedmon and Nelson, 2014). Spring and autumn blooms in NRE could explain why intercepts of seasonal regression models for DOC vs. a_{350} were often larger than in summer and winter (Table 4; Pinckney et al., 1998). Estuarine systems in which long residence time allows for substantial primary production can add a planktonic component to the overall estuarine CDOM signal (Fellman et al., 2011; Osburn et al., 2012). Evidence of this phenomenon likely explains the NRE results which were the most variable of estuaries studied here. Intertidal production of DOC is probably low in this microtidal estuary, but was observed in the Gironde estuary, which also has internal production of CDOM, further complicating optical-biogeochemical models (Abril et al., 2002; Huguet et al., 2009). Together, for NRE, these effects caused a

disruption of classic binary mixing between river and seawater that underlay the robust CDOM-DOC and CDOM-lignin relationships found by Fichot and Benner (2012) for the MARS.

Similar to NRE, the CBE exhibited large seasonal variability in CDOM-DOC and CDOM-lignin relationships. Direct evidence of phytoplankton production of CDOM in the Chesapeake Bay has been less well documented (Rochelle-Newall and Fisher, 2002). CBE also has multiple sub-estuaries flowing into it and rivers of these sub-estuaries have 50–80% more DOC than the Susquehanna River, which is the main tributary to CBE (Raymond and Bauer, 2000). Thus, it was not surprising that seasonal and interannual variability were also important to this estuary. We lacked sufficient observations from the Potomac River and York River estuaries, which comprise large amounts of flow to the lower CBE. A focus on these systems might improve the overall picture with respect to CDOM, DOC, and lignin dynamics in the CBE as well as parse out commonalities among eutrophic estuaries in contrast to LDEs.

CONCLUSIONS

This work has narrowed the knowledge gap between CDOM-DOC and CDOM-lignin relationships that have been developed for large rivers and coastal waters by focusing specifically on estuaries, which are notoriously heterogeneous. We found that both DOC and lignin can be quantified with CDOM absorption with roughly 75% certainty across several estuary types. CDOM fluorescence suggested that the dominant source of CDOM in the estuaries and coastal waters we studied was terrestrial inputs. Hydrologic variability in river flow appeared to be the dominant control on the linkage of CDOM and DOC we observed in these estuaries—and showed the major influence of terrestrial DOM.

1369 High river flow contributed more CDOM and lignin. Low river
1370 flow and longer residence time within the estuary allowed for
1371 planktonic contributions to DOM. Much of the variability in
1372 DOM quality likely is explained by the history of this material in
1373 the soil organic matter pool and any subsequent biogeochemical
1374 processing across the terrestrial-marine continuum (Marín-
1375 Spiotta et al., 2014).

1376 It was beyond the scope of this study to compute yields of
1377 terrestrial (or planktonic) DOC from these estuaries, but the
1378 models developed may be scaled to remote sensing platforms
1379 in space and *in situ* observatories (e.g., Mannino et al., 2008;
1380 Etheridge et al., 2014; Osburn et al., 2015). Wide variability in
1381 the models among these estuaries thus suggested that local or
1382 regional models should be developed for prediction of terrestrial
1383 DOM fluxes into the coastal ocean using optical properties. A one
1384 size fits all approach is not appropriate for estuaries collectively,
1385 but possible for classes of estuaries (e.g., large delta front vs.
1386 coastal plain) (Asmala et al., 2012). Upscaling to remotely sensed
1387 observations are entirely possible yet must require optimization
1388 of basic equations based on calibration and validation data sets.
1389 Results from such work will continue to spur new questions,
1390 hopefully integrating other disciplines, such as meteorology and
1391 climatology, and ultimately leading to a greater understanding of
1392 organic matter sources and cycling in coastal waters.
1393

1394 AUTHOR CONTRIBUTIONS

1395 CO conceived of this manuscript, analyzed data, and lead the
1396 writing. TB provided data analysis, co-wrote, and assisted in data
1397 collection. MM and RC co-wrote and assisted in data collection.
1398 TB and HP contributed data and co-wrote.
1399

1400 REFERENCES

- 1401 Amon, R. M. W., Budéus, G., and Meon, B. (2003). Dissolved organic carbon
1402 distribution and origin in the Nordic Seas: exchanges with the Arctic Ocean
1403 and the North Atlantic. *J. Geophys. Res.* 108, 3221. doi: 10.1029/2002jc001594
1404
1405 Amon, R. M. W., Rinehart, A. J., Duan, S., Louchouart, P., Prokushkin, A.,
1406 Guggenberger, G., et al. (2012). Dissolved organic matter sources in large Arctic
1407 rivers. *Geochim. Cosmochim. Acta* 94, 217–237. doi: 10.1016/j.gca.2012.07.015
1408
1409 Asmala, E., Stedmon, C. A., and Thomas, D. N. (2012). Linking CDOM spectral
1410 absorption to dissolved organic carbon concentrations and loadings in boreal
1411 estuaries. *Estuar. Coast. Shelf Sci.* 111, 107–117. doi: 10.1016/j.ecss.2012.06.015
1412
1413 Bianchi, T. S. (2007). *Biogeochemistry of Estuaries*. Oxford University Press, 720.
1414
1415 Bianchi, T. S., DiMarco, S. F., Smith, R. W., and Schreiner, K. M. (2009). A
1416 gradient of dissolved organic carbon and lignin from Terrebonne-Timbalier
1417 Bay Estuary to the Louisiana Shelf (USA). *Mar. Chem.* 117, 32–41. doi:
1418 10.1016/j.marchem.2009.07.010
1419
1420 Bianchi, T. S., Garcia-Tigreros, F., Yvon-Lewis, S. A., Shields, M., Mills, H. J.,
1421 Butman, D., et al. (2013). Enhanced transfer of terrestrially derived carbon
1422 to the atmosphere in a flooding event. *Geophys. Res. Lett.* 40, 116–122. doi:
1423 10.1029/2012GL054145
1424
1425 Boyd, T. J., and Osburn, C. L. (2004). Changes in CDOM fluorescence
1426 from allochthonous and autochthonous sources during tidal mixing and
1427 bacterial degradation in two coastal estuaries. *Mar. Chem.* 89, 189–210. doi:
1428 10.1016/j.marchem.2004.02.012
1429
1430 Boyle, E. S., Guerriero, N., Thiallet, A., Del Vecchio, R., and Blough, N. V. (2009).
1431 Optical properties of humic substances and CDOM: relation to structure.
1432 *Environ. Sci. Technol.* 43, 2262–2268. doi: 10.1021/es803264g

1426 FUNDING

1427 The following agencies are thanked for their financial support:
1428 Strategic Environmental Research and Development Program,
1429 ER-1431 and ER-2124 (MM, CO); North Carolina Department of
1430 Environment and Natural Resources, Contract #4443 (HP, CO);
1431 and the Lower Neuse Basin Association (HP).
1432

1433 ACKNOWLEDGMENTS

1434 We thank the following people for technical support during
1435 the field and laboratory work done for this study: Tiffanee
1436 Donowick, Erin Kelley, Jeff Denzel, Mike Shields, Lauren
1437 Handsel, and Jennifer Dixon. Special thanks to Warwick
1438 Vincent for logistical support for the Mackenzie River Estuary
1439 sampling. We also thank the captains and crews of the following
1440 vessels that were used to assemble this data set: *RV Cape*
1441 *Henlopen*, *RV John Sharp*, *RV Cape Hatteras*, *RV Barnes*, *CCGS*
1442 *Nahidik*, and *RV Pelican*. The following agencies are thanked
1443 for their financial support: Office of Naval Research (CO,
1444 TB, RC), Strategic Environmental Research and Development
1445 Program (MM, CO), NASA (CO, TB), and National Science
1446 Foundation (HP), and the NC Dept. of Environment
1447 and Natural Resources-Lower Neuse Basin Association
1448 (HP, CO).
1449
1450

1451 SUPPLEMENTARY MATERIAL

1452 The Supplementary Material for this article can be found
1453 online at: <http://journal.frontiersin.org/article/10.3389/fmars.2015.00127>
1454

- 1455
1456
1457
1458
1459
1460 Coble, P. G. (1996). Characterization of marine and terrestrial DOM in seawater
1461 using excitation emission matrix spectroscopy. *Mar. Chem.* 51, 325–346. doi:
1462 10.1016/0304-4203(95)00062-3
1463
1464 Coble, P. G. (2007). Marine optical biogeochemistry: the chemistry of ocean color.
1465 *Chem. Rev.* 107, 402–418. doi: 10.1021/cr050350+
1466
1467 Cory, R. M., Miller, M. P., McKnight, D. M., Guerard, J. J., and Miller,
1468 P. L. (2010). Effect of instrument-specific response on the analysis of
1469 fulvic acid fluorescence spectra. *Limnol. Oceanogr. Methods* 8, 67–78. doi:
1470 10.4319/lom.2010.8.0067
1471
1472 Del Vecchio, R., and Blough, N. V. (2004). On the origin of the optical
1473 properties of humic substances. *Environ. Sci. Technol.* 38, 3885–3891. doi:
1474 10.1021/es049912h
1475
1476 Dixon, J. L. (2014). *Seasonal Changes in Estuarine Dissolved Organic Matter Due to*
1477 *Variations in Discharge, Flushing Times and Wind-driven Mixing Events*. Ph.D.
1478 thesis, North Carolina State University.
1479
1480 Etheridge, J. R., Birgand, F., Osborne, J. A., Osburn, C. L., Burchell, M. R., and
1481 Irving, J. (2014). Using *in situ* ultraviolet–visual spectroscopy to measure
1482 nitrogen, carbon, phosphorus, and suspended solids concentrations at a high
1483 frequency in a brackish tidal marsh. *Limnol. Oceanogr. Methods* 12, 10–22. doi:
1484 10.4319/lom.2014.12.10
1485
1486 Fellman, J. B., Petrone, K. C., and Grierson, P. F. (2011). Source, biogeochemical
1487 cycling, and fluorescence characteristics of dissolved organic matter in an agro-
1488 urban estuary. *Limnol. Oceanogr.* 56, 243–256. doi: 10.4319/lo.2011.56.1.0243
1489
1490 Ferrari, G. M. (2000). The relationship between chromophoric dissolved organic
1491 matter and dissolved organic carbon in the European Atlantic coastal area and
1492 in the West Mediterranean Sea (Gulf of Lions). *Mar. Chem.* 70, 339–357. doi:
1493 10.1016/S0304-4203(00)00036-0
1494
1495

- Fichot, C. G., and Benner, R. (2011). A novel method to estimate DOC concentrations from CDOM absorption coefficients in coastal waters. *Geophys. Res. Lett.* 38. doi: 10.1029/2010GL046152
- Fichot, C. G., and Benner, R. (2012). The spectral slope coefficient of chromophoric dissolved organic matter (S_{275–295}) as a tracer of terrigenous dissolved organic carbon in river-influenced ocean margins. *Limnol. Oceanogr.* 57, 1453–1466. doi: 10.4319/lo.2012.57.5.1453
- Fichot, C. G., Lohrenz, S. E., and Benner, R. (2014). Pulsed, cross-shelf export of terrigenous dissolved organic carbon to the Gulf of Mexico. *J. Geophys. Res. Oceans* 119. doi: 10.1002/2013jc009424
- Goñi, M. A., and Montgomery, S. (2000). Alkaline CuO oxidation with a microwave digestion system: lignin analyses of geochemical samples. *Anal. Chem.* 72, 3116–3121. doi: 10.1021/ac991316w
- Gonsior, M., Peake, B. M., Cooper, W. T., Podgorski, D., D'Andrilli, J., and Cooper, W. J. (2009). Photochemically induced changes in dissolved organic matter identified by ultrahigh resolution Fourier transform ion cyclotron resonance mass spectrometry. *Environ. Sci. Technol.* 43, 698–703. doi: 10.1021/es8022804
- Goodwin, T. W., and Mercer, E. I. (1972). *Introduction to Plant Biochemistry*. New York, NY: Pergamon Press.
- Helms, J. R., Stubbins, A., Ritchie, J. D., Minor, E. C., Kieber, D. J., and Mopper, K. (2008). Absorption spectral slopes and slope ratios as indicators of molecular weight, source, and photobleaching of chromophoric dissolved organic matter. *Limnol. Oceanogr.* 53:955. doi: 10.4319/lo.2008.53.3.0955
- Hernes, P. J., and Benner, R. (2003). Photochemical and microbial degradation of dissolved lignin phenols: implications for the fate of terrigenous dissolved organic matter in marine environments. *J. Geophys. Res. Oceans (1978–2012)* 108. doi: 10.1029/2002jc001421
- Hernes, P. J., Bergamaschi, B. A., Eckard, R. S., and Spencer, R. G. M. (2009). Fluorescence-based proxies for lignin in freshwater dissolved organic matter. *J. Geophys. Res.* 114, G00F03. doi: 10.1029/2009JG000938
- Hernes, P. J., Robinson, A. C., and Aufdenkampe, A. K. (2007). Fractionation of lignin during leaching and sorption and implications for organic matter “freshness.” *Geophys. Res. Lett.* 34, L17401. doi: 10.1029/2007GL031017
- Hernes, P. J., Spencer, R. G., Dyda, R. Y., Pellerin, B. A., Bachand, P. A., and Bergamaschi, B. A. (2008). The role of hydrologic regimes on dissolved organic carbon composition in an agricultural watershed. *Geochim. Cosmochim. Acta* 72, 5266–5277. doi: 10.1016/j.gca.2008.07.031
- Huguet, A., Vacher, L., Relexans, S., Saubusse, S., Froidefond, J. M., and Parlanti, E. (2009). Properties of fluorescent dissolved organic matter in the Gironde Estuary. *Org. Geochem.* 40, 706–719. doi: 10.1016/j.orggeochem.2009.03.002
- Kaiser, K., and Benner, R. (2011). Characterization of lignin by gas chromatography and mass spectrometry using a simplified CuO oxidation method. *Anal. Chem.* 84, 459–464. doi: 10.1021/ac202004r
- Lønborg, C., Álvarez-Salgado, X. A., Davidson, K., Martínez-García, S., and Teira, E. (2010). Assessing the microbial bioavailability and degradation rate constants of dissolved organic matter by fluorescence spectroscopy in the coastal upwelling system of the Ría de Vigo. *Mar. Chem.* 119, 121–129. doi: 10.1016/j.marchem.2010.02.001
- Louchouart, P., Opsahl, S., and Benner, R. (2000). Isolation and quantification of dissolved lignin from natural waters using solid-phase extraction and GC/MS. *Anal. Chem.* 72, 2780–2787. doi: 10.1021/ac9912552
- Mannino, A., Russ, M. E., and Hooker, S. B. (2008). Algorithm development and validation for satellite-derived distributions of DOC and CDOM in the US Middle Atlantic Bight. *J. Geophys. Res. Oceans (1978–2012)* 113, C07051. doi: 10.1029/2007JC004493
- Marin-Spiotta, E., Gruley, K. E., Crawford, J., Atkinson, E. E., Miesel, J. R., Greene, S., et al. (2014). Paradigm shifts in soil organic matter research affect interpretations of aquatic carbon cycling: transcending disciplinary and ecosystem boundaries. *Biogeochemistry* 117, 279–297. doi: 10.1007/s10533-013-9949-7
- McCallister, S. L., Bauer, J. E., Cherrier, J. E., and Ducklow, H. W. (2004). Assessing sources and ages of organic matter supporting river and estuarine bacterial production: a multiple-isotope ($\Delta^{14}\text{C}$, $\delta^{13}\text{C}$, and $\delta^{15}\text{N}$) approach. *Limnol. Oceanogr.* 49, 1687–1702. doi: 10.4319/lo.2004.49.5.1687
- Miller, W. L., and Moran, M. A. (1997). Interaction of photochemical and microbial processes in the degradation of refractory dissolved organic matter from a coastal marine environment. *Limnol. Oceanogr.* 42, 1317–1324. doi: 10.4319/lo.1997.42.6.1317
- Moran, M. A., Sheldon, W. M., and Zepp, R. G. (2000). Carbon loss and optical property changes during long-term photochemical and biological degradation of estuarine dissolved organic matter. *Limnol. Oceanogr.* 45, 1254–1264. doi: 10.4319/lo.2000.45.6.1254
- Murphy, K. R., Stedmon, C. A., Graeber, D., and Bro, R. (2013). Fluorescence spectroscopy and multi-way techniques. *PARAFAC. Anal. Methods* 5, 6557–6566. doi: 10.1039/c3ay41160e
- Onstad, G. D., Canfield, D. E., Quay, P. D., and Hedges, J. I. (2000). Sources of particulate organic matter in rivers from the continental USA: lignin phenol and stable carbon isotope compositions. *Geochim. Cosmochim. Acta* 64, 3539–3546. doi: 10.1016/S0016-7037(00)00451-8
- Osburn, C. L., Del Vecchio, R., and Boyd, T. J. (2014). “Physicochemical effects on dissolved organic matter fluorescence in natural waters,” in *Aquatic Organic Matter Fluorescence*, eds A. Baker, P. G. Coble, J. R. Lead, D. Reynolds, and R. G. M. Spencer (Cambridge University Press).
- Osburn, C. L., Handsel, L. T., Mikan, M. P., Paerl, H. W., and Montgomery, M. T. (2012). Fluorescence tracking of dissolved and particulate organic matter quality in a river-dominated estuary. *Environ. Sci. Technol.* 46, 8628–8636. doi: 10.1021/es3007723
- Osburn, C. L., Mikan, M. P., Etheridge, J. R., Burchell, M. R., and Birgand, F. (2015). Seasonal variation in the quality of dissolved and particulate organic matter exchanged between a salt marsh and its adjacent estuary. *J. Geophys. Res. Biogeosci.* 120, 1430–1449. doi: 10.1002/2014jg002897
- Osburn, C. L., Retamal, L., and Vincent, W. F. (2009). Photoreactivity of chromophoric dissolved organic matter transported by the Mackenzie River to the Beaufort Sea. *Mar. Chem.* 115, 10–20. doi: 10.1016/j.marchem.2009.05.003
- Osburn, C. L., and Stedmon, C. A. (2011). Linking the chemical and optical properties of dissolved organic matter in the Baltic–North Sea transition zone to differentiate three allochthonous inputs. *Mar. Chem.* 126, 281–294. doi: 10.1016/j.marchem.2011.06.007
- Osburn, C. L., and St-Jean, G. (2007). The use of wet chemical oxidation with high-amplification isotope ratio mass spectrometry (WCO–IRMS) to measure stable isotope values of dissolved organic carbon in seawater. *Limnol. Oceanogr. Methods* 5, 296–308. doi: 10.4319/lom.2007.5.296
- Paerl, H. W. (2009). Controlling eutrophication along the freshwater–marine continuum: dual nutrient (N and P) reductions are essential. *Estuar. Coast.* 32, 593–601. doi: 10.1007/s12237-009-9158-8
- Paerl, H. W., Pinckney, J. L., Fear, J. M., and Peierls, B. L. (1998). Ecosystem responses to internal and watershed organic matter loading: consequences for hypoxia in the eutrophying Neuse River Estuary, North Carolina, USA. *Mar. Ecol. Prog. Ser.* 166:17. doi: 10.3354/meps166017
- Paerl, H. W., Valdes, L. M., Peierls, B. L., Adolf, J. E., and Harding, L. Jr. (2006). Anthropogenic and climatic influences on the eutrophication of large estuarine ecosystems. *Limnol. Oceanogr.* 51, 448–462. doi: 10.4319/lo.2006.51.1_part_2.0448
- Pinckney, J. L., Paerl, H. W., Harrington, M. B., and Howe, K. E. (1998). Annual cycles of phytoplankton community-structure and bloom dynamics in the Neuse River Estuary, North Carolina. *Mar. Biol.* 131, 371–381. doi: 10.1007/s002270050330
- Raymond, P. A., and Bauer, J. E. (2000). Bacterial consumption of DOC during transport through a temperate estuary. *Aquat. Microb. Ecol.* 22, 1–12. doi: 10.3354/ame022001
- Raymond, P. A., and Spencer, R. G. M. (2014). “Riverine DOM,” in *Biogeochemistry of Marine Dissolved Organic Matter, 2nd Edn.*, eds D. A. Hansell and C. A. Carlson (Academic Press), 509–535.
- Rochelle-Newall, E. J., and Fisher, T. R. (2002). Chromophoric dissolved organic matter and dissolved organic carbon in Chesapeake Bay. *Mar. Chem.* 77, 23–41. doi: 10.1016/S0304-4203(01)00073-1
- Romera-Castillo, C., Sarmiento, H., Alvarez-Salgado, X. A., Gasol, J. M., and Marrasé, C. (2011). Net production and consumption of fluorescent colored dissolved organic matter by natural bacterial assemblages growing on marine phytoplankton exudates. *Appl. Environ. Microbiol.* 77, 7490–7498. doi: 10.1128/AEM.00200-11
- Saraceno, J. F., Pellerin, B. A., Downing, B. D., Boss, E., Bachand, P. A., and Bergamaschi, B. A. (2009). High-frequency *in situ* optical measurements during a storm event: assessing relationships between dissolved organic matter, sediment concentrations, and hydrologic processes. *J. Geophys. Res. Biogeosci.* (2005–2012) 114. doi: 10.1029/2009jg000989

- 1597 Senesi, N. (1990). Molecular and quantitative aspects of the chemistry of fulvic acid
1598 and its interactions with metal ions and organic chemicals. 2. The fluorescence
1599 spectroscopy approach. *Anal. Chim. Acta* 232, 77–106. doi: 10.1016/S0003-
1600 2670(00)81226-X
- 1601 Spencer, R. G., Aiken, G. R., Dornblaser, M. M., Butler, K. D., Holmes, R. M., Fiske,
1602 G., et al. (2013). Chromophoric dissolved organic matter export from US rivers.
1603 *Geophys. Res. Lett.* 40, 1575–1579. doi: 10.1002/grl.50357
- 1604 **Q16** Spencer, R. G., Aiken, G. R., Wickland, K. P., Striegl, R. G., and Hernes, P. J.
1605 (2008). Seasonal and spatial variability in dissolved organic matter quantity and
1606 composition from the Yukon River basin, Alaska. *Glob. Biogeochem. Cycles* 22.
1607 doi: 10.1029/2008GB003231
- 1608 Spencer, R. G., Butler, K. D., and Aiken, G. R. (2012). Dissolved organic carbon
1609 and chromophoric dissolved organic matter properties of rivers in the USA.
1610 *J. Geophys. Res. Biogeosci.* (2005–2012) 117, G03001. doi: 10.1029/2011jg
1611 001928
- 1612 Spencer, R. G., Hernes, P. J., Ruf, R., Baker, A., Dyda, R. Y., Stubbins, A.,
1613 et al. (2010). Temporal controls on dissolved organic matter and lignin
1614 biogeochemistry in a pristine tropical river, Democratic Republic of Congo.
1615 *J. Geophys. Res. Biogeosci.* (2005–2012) 115, G03013. doi: 10.1029/2009jg
1616 001180
- 1617 Stedmon, C. A., and Markager, S. (2005). Tracing the production and degradation
1618 of autochthonous fractions of dissolved organic matter by fluorescence analysis.
1619 *Limnol. Oceanogr.* 50, 1415–1426. doi: 10.4319/lo.2005.50.5.1415
- 1620 Stedmon, C. A., Markager, S., and Kaas, H. (2000). Optical properties and
1621 signatures of chromophoric dissolved organic matter (CDOM) in Danish
1622 coastal waters. *Estuar. Coast. Shelf Sci.* 51, 267–278. doi: 10.1006/ecss.2000.0645
- 1623 Stedmon, C. A., and Nelson, N. B. (2014). “The optical properties of DOM in the
1624 ocean,” in *Biogeochemistry of Marine Dissolved Organic Matter, 2nd Edn.*, eds D.
1625 A. Hansell and C. A. Carlson (Academic Press), 509–535.
- 1626 Tehrani, N. C., D’Sa, E. J., Osburn, C. L., Bianchi, T. S., and Schaeffer, B. A.
1627 (2013). Chromophoric dissolved organic matter and dissolved organic carbon
1628 from sea-viewing wide field-of-view sensor (SeaWiFS), Moderate Resolution
1629 Imaging Spectroradiometer (MODIS) and MERIS Sensors: case study for the
1630 Northern Gulf of Mexico. *Remote Sens.* 5, 1439–1464. doi: 10.3390/rs5031439
- 1631 Tzortziou, M., Neale, P. J., Osburn, C. L., Megonigal, J. P., Maie, N., and Jaffé,
1632 R. (2008). Tidal marshes as a source of optically and chemically distinctive
1633 colored dissolved organic matter in the Chesapeake Bay. *Limnol. Oceanogr.* 53,
1634 148–159. doi: 10.4319/lo.2008.53.1.0148
- 1635 Uher, G., Hughes, C., Henry, G., and Upstill-Goddard, R. C. (2001).
1636 Non-conservative mixing behavior of colored dissolved organic matter
1637 in a humic-rich, turbid estuary. *Geophys. Res. Lett.* 28, 3309–3312. doi:
1638 10.1029/2000GL012509
- 1639 Walker, S. A., Amon, R. M., Stedmon, C., Duan, S., and Louchouart, P. (2009).
1640 **Q18** The use of PARAFAC modeling to trace terrestrial dissolved organic matter and
1641 fingerprint water masses in coastal Canadian Arctic surface waters. *J. Geophys.*
1642 *Res. Biogeosci.* (2005–2012). doi: 10.1029/2009jg000990
- 1643 Walker, S. A., Amon, R. M., and Stedmon, C. A. (2013). Variations in high-latitude
1644 riverine fluorescent dissolved organic matter: a comparison of large Arctic
1645 rivers. *J. Geophys. Res. Biogeosci.* 118, 1689–1702. doi: 10.1002/2013JG002320
- 1646 Weishaar, J. L., Aiken, G. R., Bergamaschi, B. A., Fram, M. S., Fujii, R., and Mopper,
1647 K. (2003). Evaluation of specific ultraviolet absorbance as an indicator of the
1648 chemical composition and reactivity of dissolved organic carbon. *Environ. Sci.*
1649 *Technol.* 37, 4702–4708. doi: 10.1021/es030360x
- 1650 Wolfbeis, O. S. (1985). “The fluorescence of organic natural products,” in *Molecular*
1651 **Q17** *Luminescence Spectroscopy Methods and Applications*, ed S. G. Schulman
1652 (Wiley).
1653 Zhang, Y., van Dijk, M. A., Liu, M., Zhu, G., and Qin, B. (2009). The contribution
1654 of phytoplankton degradation to chromophoric dissolved organic matter
1655 (CDOM) in eutrophic shallow lakes: field and experimental evidence. *Water*
1656 *Res.* 43, 4685–4697. doi: 10.1016/j.watres.2009.07.024
- 1657 **Conflict of Interest Statement:** The authors declare that the research was
1658 conducted in the absence of any commercial or financial relationships that could
1659 be construed as a potential conflict of interest.
- 1660
1661
1662
1663
1664
1665
1666
1667
1668
1669
1670
1671
1672
1673
1674
1675
1676
1677
1678
1679
1680
1681
1682
1683
1684
1685
1686
1687
1688
1689
1690
1691
1692
1693
1694
1695
1696
1697
1698
1699
1700
1701
1702
1703
1704
1705
1706
1707
1708
1709
1710